

## Corotating Magnetospheric Convection

T. W. HILL, A. J. DESSLER, AND L. J. MAHER

*Space Physics and Astronomy Department, Rice University, Houston, Texas 77001*

The longitudinal asymmetry of the Io plasma torus, as predicted by the magnetic-anomaly model and observed by Earth-based optical astronomy, provides a driving mechanism for a corotating convection system in Jupiter's magnetosphere. Here we deduce some qualitative properties of this convection system from the general equations that govern a steady state corotating convection system (although we expect that time-dependent effects may also have to be included for a complete description of Jovian convection). The corotating convection system appears capable of providing both the dominant radial transport mechanism (with a time scale possibly as short as a few rotation periods) and the dominant mechanism for extracting energy from Jupiter's rotation (at a rate  $\sim 10^{15}$  W) for driving a wide variety of magnetospheric phenomena. A similar corotating convection system may occur in other rotation-dominated magnetospheres, for example, those of pulsars and Saturn.

### INTRODUCTION

Several lines of evidence suggest that Jupiter's magnetosphere possesses a persistent longitudinal asymmetry that corotates with Jupiter [e.g., Hill et al., 1974b; Vasyliunas, 1975; Carbary et al., 1976; Fillius and Knickerbocker, 1979, Vasyliunas and Dessler, 1981]. In particular, recent Earth-based optical observations have demonstrated a significant longitudinal asymmetry in the torus of plasma that surrounds Jupiter near the orbit of Io (as seen in the collisionally excited emission lines of singly ionized sulfur) [Trafton, 1980; Pilcher and Morgan, 1980; Trauger et al., 1980]. This asymmetry is explained by the existence of an 'active sector,' a restricted range of longitude in which the rate of plasma production in the magnetosphere is enhanced by processes related to the longitudinal asymmetry of Jupiter's intrinsic magnetic field [Dessler and Hill, 1975, 1979; Hill and Dessler, 1976].

It was initially pointed out by Vasyliunas [1978] that such an azimuthally asymmetric plasma mass distribution will spontaneously generate a convection system with outward flow (away from Jupiter) in the longitude sector having greater-than-average plasma mass density, and inward return flow in the longitude sector having less-than-average mass density. This convection system, like the asymmetry that drives it, is fixed in the corotating Jovian frame of reference. Thus it differs in two important respects from the solar-wind-driven convection that is known to occur in Earth's magnetosphere: (1) the Jovian system is powered by internal, rather than external, sources of plasma and energy; and (2) the convection pattern is fixed in the (rotating) Jovian reference frame rather than in the (inertial) solar-wind reference frame.

In this paper we describe qualitatively the global nature of this convection system and deduce a semiquantitative estimate of the convection time scale. The estimated convection time scale is comparable to a few Jovian rotation periods, and hence we conclude that convection represents the dominant radial transport process in the Jovian magnetosphere. An important additional conclusion is that both the Jovian ionospheric conductivity and the plasma injection rate in the Io plasma torus must be considerably larger than previous estimates in order to make the estimated convection time scale consistent with observations and with previous theoretical work. A self-consistent treatment of the convection problem

requires the solution of a pair of coupled nonlinear partial differential equations, which we derive here but do not solve.

Chen [1977] has studied the related problem of outward convection generated by the mass loading of flux tubes in the immediate vicinity of Io and has concluded that such convection is an unimportant radial transport mechanism. Our conclusion differs from Chen's fundamentally because we consider the azimuthal asymmetry that drives the convection to be fixed in Jovian (System III) longitude [e.g., Vasyliunas, 1978; Dessler and Hill, 1975, 1979] so that its effects are cumulative over several Jovian rotations, whereas Chen considered the asymmetry to be fixed in relation to Io such that its effect is felt at a given longitude for only a fraction of one Jovian rotation period. (Another, less fundamental, difference is that we adopt a larger mass-loading rate than that used by Chen, led by recent Voyager and astronomical measurements.) However, Chen's mathematical formulation of the problem is formally similar to that presented here, the main differences being in the choice of approximations and boundary conditions.

We base our model on the assumption that the immediate source of magnetospheric plasma is not Io itself but rather a more-or-less complete torus of neutral gas (mostly SO<sub>2</sub> and its dissociation products) that orbits Jupiter near the orbit of Io. The neutral gas cloud is ultimately supplied by Io, but its presence at a given longitude is independent of the instantaneous position of Io in its orbit.

### GOVERNING EQUATIONS

In the corotating frame of reference the torus plasma experiences an outward centrifugal force that is largely balanced by the  $\mathbf{j} \times \mathbf{B}$  force associated with the acceleration drift current  $\mathbf{j}$ . Beyond the orbit of Io at 6  $R_J$  distance ( $R_J$  = Jupiter's radius) the force of Jupiter's gravity is negligible compared to the corotational centrifugal force. The steady state force-balance equation is thus

$$\rho \mathbf{v} \cdot \nabla \mathbf{v} = \rho \Omega^2 \mathbf{r} - 2\rho \Omega \times \mathbf{v} + \mathbf{j} \times \mathbf{B} - \nabla p \quad (1)$$

where  $\rho$  is plasma mass density,  $\mathbf{v}$  is its bulk velocity with respect to the corotating frame,  $\Omega$  is the angular frequency of corotation, and  $\mathbf{r}$  is the axial radius vector in a cylindrical ( $r, \theta, z$ ) coordinate system aligned with the rotation axis. (In its more familiar form, the MHD force-balance equation is written in terms of the velocity  $\mathbf{v}' = \mathbf{v} + \Omega \times \mathbf{r}$  as measured in the nonrotating reference frame. In this frame, the centrifugal and Coriolis forces (first two terms on the right-hand side of (1))

are included implicitly in the inertial term (left-hand side.) We shall neglect the pressure-gradient force  $-\nabla p$ ; this is equivalent to assuming that the plasma is cold in the sense  $kT \lesssim m\Omega^2 r^2/2$ . (The pressure-gradient current has the same direction and the same longitudinal asymmetry as the centrifugal-acceleration current, so the inclusion of the pressure-gradient force, while complicating the problem considerably, would not change the qualitative nature of the result and would alter the quantitative result by at most a factor of the order of two [see Dessler, 1980a].) We further assume that the plasma is largely confined to a thin equatorial sheet (sufficiently thin that  $\mathbf{B}$  and  $\mathbf{v}$  have essentially their equatorial values throughout the thickness of the sheet)—(1) can then be integrated across the sheet thickness to give

$$\sigma \mathbf{v} \cdot \nabla \mathbf{v} \approx \sigma \Omega^2 \mathbf{r} - 2\sigma \boldsymbol{\Omega} \times \mathbf{v} + \mathbf{J} \times \mathbf{B} \quad (2)$$

where  $J = \int j dz$  and  $\sigma = \int \rho dz$ ;  $\sigma$  is thus the mass density per unit equatorial area. We further assume that  $\mathbf{v}$  obeys the frozen-in-flux approximation

$$\mathbf{E} + \mathbf{v} \times \mathbf{B} = 0 \quad (3)$$

where, in accordance with our steady state assumption, the electric field is derivable from a scalar potential:

$$\mathbf{E} = -\nabla \Phi \quad (4)$$

The velocity is thus a function of the potential:

$$\mathbf{v} = \mathbf{B} \times \nabla \Phi / B^2 \quad (5)$$

Upon substituting (5) into (2) we find that the force-balance equation (2) contains the four unknown functions  $\sigma$ ,  $\Phi$ ,  $J_r$ , and  $J_\theta$ . (The field  $\mathbf{B}$  is assumed to be given.) The two functions  $\sigma$  and  $\Phi$  are further related by the mass continuity equation

$$\nabla \cdot (\rho \mathbf{v}) = 0 \quad (6)$$

which translates to

$$\mathbf{v} \cdot \nabla \eta = 0 \quad (7)$$

where  $\eta = \sigma/B$  is the mass per unit magnetic flux, which according to (7) is conserved along streamlines. Utilizing (5), (7) can be written

$$\frac{\partial \Phi}{\partial r} \frac{\partial \eta}{\partial \theta} - \frac{\partial \Phi}{\partial \theta} \frac{\partial \eta}{\partial r} = 0 \quad (8)$$

It remains now to eliminate  $\mathbf{J}$  from (2); this is accomplished by imposing the current-continuity equation

$$\nabla \cdot \mathbf{j} = 0 \quad (9)$$

Thus the divergence of the equatorial magnetospheric current must, in a steady state, be compensated by Birkeland (magnetic-field-aligned) currents, and the closure of these Birkeland currents through Jupiter's ionosphere imposes a relationship between  $\mathbf{E}$  and  $\mathbf{J}$  both in the ionosphere and (through (3)) also in the equatorial plane. (The same procedure is widely used in computing the effects of ionospheric conductivity on terrestrial magnetospheric convection, see, for example, Vasylunas [1970]; Wolf [1970].) The relationship, derived in the Appendix, is

$$\frac{\partial}{\partial r} (rJ_r) + \frac{\partial}{\partial \theta} (J_\theta) = -4\Sigma \frac{\partial}{\partial r} (rE_r) - \Sigma \frac{\partial}{\partial \theta} (E_\theta) \quad (10)$$

where  $\Sigma$ , the height-integrated Pedersen conductivity of Jupi-

ter's ionosphere, is assumed to be uniform over Jupiter's surface. The derivation of (10) applies to a spin-aligned dipole magnetic field and utilizes the approximation  $(1 - 1/L)^{1/2} \approx 1$ , where  $L = r/R_J$ .

If we now evaluate  $J_r$  and  $J_\theta$  from (2) and insert in (10), there results a second differential equation relating  $\eta$  and  $\Phi$ :

$$\begin{aligned} & \Sigma B_J^2 R_J^6 \left[ 4 \frac{\partial}{\partial r} \left( r \frac{\partial \Phi}{\partial r} \right) + \frac{\partial}{\partial \theta} \left( \frac{1}{r} \frac{\partial \Phi}{\partial \theta} \right) \right] \\ &= \frac{\partial}{\partial r} \left\{ r^3 \eta \left[ 2\Omega B_J R_J^3 \frac{\partial \Phi}{\partial \theta} + \frac{\partial \Phi}{\partial r} \frac{\partial}{\partial \theta} \left( r^2 \frac{\partial \Phi}{\partial r} \right) - \frac{\partial \Phi}{\partial \theta} \frac{\partial}{\partial r} \left( r^2 \frac{\partial \Phi}{\partial r} \right) \right] \right\} \\ &+ \frac{\partial}{\partial \theta} \left\{ r \eta \left[ \Omega^2 B_J^2 R_J^6 - 2\Omega B_J R_J^3 r^2 \frac{\partial \Phi}{\partial r} - r \frac{\partial \Phi}{\partial \theta} \frac{\partial}{\partial r} \left( r^2 \frac{\partial \Phi}{\partial \theta} \right) \right. \right. \\ &\quad \left. \left. + r \frac{\partial \Phi}{\partial r} \frac{\partial}{\partial \theta} \left( r^2 \frac{\partial \Phi}{\partial \theta} \right) \right] \right\} \quad (11) \end{aligned}$$

In principal, both  $\eta(r, \theta)$  and  $\Phi(r, \theta)$  are completely determined by the two coupled equations, (8) and (11), given appropriate boundary conditions, and either  $\eta(r, \theta)$  or  $\Phi(r, \theta)$  serves to specify completely the convection pattern resulting from a given set of boundary conditions (both are constant along streamlines). In practice, we have not discovered any analytic technique useful for the solution of (8) and (11); their solution for a given set of boundary conditions will evidently require extensive numerical integrations, which we do not pursue in this paper. The ultimate solution to this problem must also take into account the likely possibility that the convection is time dependent, i.e., the convection velocity varies appreciably during the time of one convection cycle.

However, some useful information may be deduced from (2) and (11) under the assumption

$$v \ll \Omega r \quad (12)$$

This assumption eliminates the inertial term on the left-hand side of (2) (which is quadratic in  $v/(\Omega r)$ ) and the Coriolis term on the right-hand side (which is linear in  $v/(\Omega r)$ ), leaving the much simpler equations

$$J_r = 0 \quad (13a)$$

$$J_\theta = \eta \Omega^2 r \quad (13b)$$

The same approximation ( $v \ll \Omega r$ ) eliminates the nonlinear terms of (11), leaving

$$4 \frac{\partial}{\partial r} \left( r \frac{\partial \Phi}{\partial r} \right) + \frac{\partial}{\partial \theta} \left( \frac{1}{r} \frac{\partial \Phi}{\partial \theta} \right) = (\Omega^2 r / \Sigma) \frac{\partial \eta}{\partial \theta} \quad (14)$$

Equation (13b) permits the following simple description of the driving force of the convection system and the mechanism of its coupling to the Jovian ionosphere. The asymmetric mass loading of the torus produces a partial ring current, wherein  $\partial \eta / \partial \theta \neq 0$  implies  $\partial J_\theta / \partial \theta \neq 0$ . This partial ring current must close in Jupiter's conducting ionosphere via connecting Birkeland currents. This is illustrated in Figure 1 for the active sector wherein  $\eta$  is above average; the sense of the current closure in this case requires an electric field whose direction corresponds (by (3)) to outward flow in this sector. The flow is inward in the opposite sector (not shown) where  $\eta$  is below average. In effect, the heavier side of the torus falls outward in the centrifugal force field, drawing the lighter side inward against the same force field. The rate of fall is controlled by the ionospheric conductivity, which is a measure of the strength of the

frictional coupling between the ionized and unionized components of the atmosphere (see below). If the ionospheric conductivity were vanishingly small, the coupling would be absent and the partial ring current would polarize so as to move outward (in the active sector) in a 'free-fall' state, presumably at something like the local rotational speed (although the local rotation speed would then itself be significantly less than its corotation value—see Hill [1979]).

#### CONVECTION TIME SCALE

In spite of the simplification accomplished by assumption (12) above, the solution of the coupled equations (8) and (14) involves considerable mathematical difficulties. We therefore simplify the problem further by neglecting the first term with respect to the second term on the left-hand side of (14). This approximation is strictly valid only in some neighborhood of the outflow symmetry streamline wherein  $v_r \gg |v_\theta|$ , and we will employ it here only to obtain an order-of-magnitude estimate of the rate of outflow.

The resulting equation can then be integrated immediately to give

$$E_\theta \sim -\Omega^2 r (\eta - \eta_0) / \Sigma \quad (15)$$

where the constant of integration  $\eta_0$  is chosen as the value of  $\eta$  at the boundary between inflow ( $E_\theta > 0$ ) and outflow ( $E_\theta < 0$ ). We shall provisionally take the maximum value of  $\eta$  along the outflow symmetry streamline to be  $\eta_m \sim 2\eta_0$ . This ratio is consistent with the optical observations of the cool (inner) torus cited in the Introduction. (We note that the Voyager UVS observations of the hot outer torus [Broadfoot et al., 1981] do not reflect the same longitudinal asymmetry as is evident in the optical observations. We do not presently have a simple explanation for this apparent paradox, either in the context of our corotating convection model or any other existing model of plasma transport. Pending such an explanation, we shall explore here the consequences of the factor-of-two asymmetry implied by the optical observations.) Thus, taking  $\eta_m = 2\eta_0$  in (15), we find the maximum outflow velocity to be

$$v_r (\eta = \eta_m) = -E_\theta (\eta = \eta_m) / B \leq \Omega^2 R_J \eta_m / (2\Sigma B_J) L^4 \quad (16)$$

The convection time scale, defined as the transit time from the source distance  $L = L_s$  to the outer boundary  $L = L_b$  (see below), is

$$\tau_c = \int_{L_s}^{L_b} \frac{R_J dL}{v_r} \geq 2\Sigma B_J / (3\Omega^2 \eta_m L_s^3) \quad (17)$$

where we have assumed  $L_b^3 \gg L_s^3$ .

Equation (17) does not by itself provide a very useful estimate of the convection time scale because of the large uncertainty in our knowledge of  $\Sigma$  and  $\eta_m$ . (Estimates of  $\Sigma$  range from a value of  $\sim 0.1$  mho in the absence of auroral particle precipitation [Dessler and Hill, 1979] to a value in the range 1–10 mho in the presence of Io torus precipitation (R. L. Thorne, private communication, 1980). There is, however, an independent way of estimating  $\tau_c$  that enables us to circumvent this difficulty.

The total mass of the outflowing plasma is given by

$$M \leq \int_{L_s}^{L_b} \eta B \pi r dr \approx \pi \eta_m B_J R_J^2 / L_s \quad (18)$$

where we have assumed that the outflow occupies a longitude sector of width  $\leq \pi$  rad. If plasma mass is produced in the

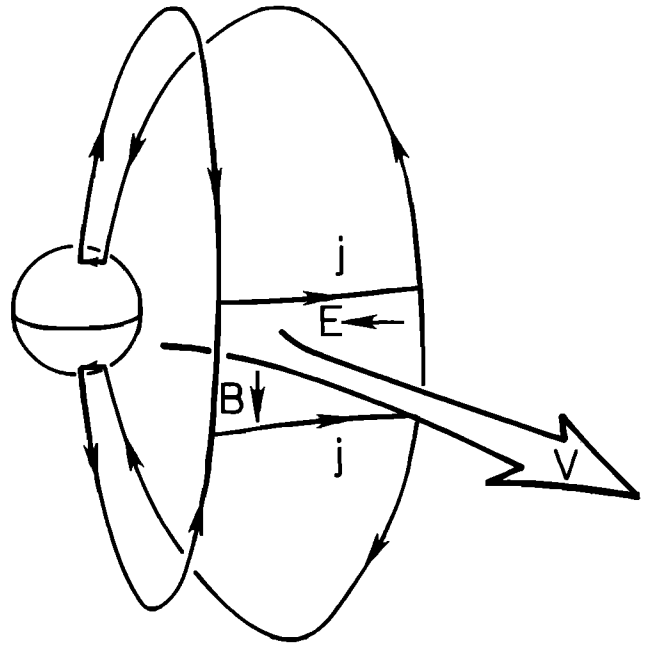


Fig. 1. Illustration of the current system associated with outflow in the active sector. The longitudinal asymmetry of plasma mass density results in a divergence of the equatorial ring current which must be compensated by Birkeland (field-aligned) currents. The ionospheric closure of these Birkeland currents, in turn, requires an electric field consistent with outward  $E \times B$  drift in the active sector.

torus at the rate  $R$  (kg/s), then the mean particle lifetime is

$$\tau_c' = M/R \leq \pi \eta_m B_J R_J^2 / (RL_s) \quad (19)$$

We now have a lower limit (17) and an upper limit (19) for the outflow time. If we assume that each limit provides a reasonable order-of-magnitude estimate, then by requiring consistency between these two estimates we arrive at the condition

$$\Sigma R \sim \frac{3\pi}{2} \eta_m^2 \Omega^2 R_J^2 L_s^2 \quad (20)$$

This result can be combined with the earlier independent result

$$\Sigma / R = L_0^4 / (\pi R_J^2 B_J^2) \quad (21)$$

where  $L_0$  represents the distance scale over which corotation breaks down [Hill, 1979]. From Voyager 1 inbound observations of plasma flow [McNutt et al., 1979], the value of  $L_0$  can be estimated [Hill, 1980] as  $L_0 \approx 20$ , with perhaps a 10% uncertainty.

Combining (20) and (21) yields

$$\Sigma \sim \sqrt{3/2} \Omega \eta_m L_s L_0^2 / B_J \quad (22)$$

$$R \sim \sqrt{3/2} \pi \Omega B_J R_J^2 \eta_m L_s / L_0^2 \quad (23)$$

Note that, at this point, we remain ignorant of the values of  $\Sigma$  and  $\eta_m$ , but we have established a reasonable estimate of their ratio (22), which is sufficient for the lifetime estimate (17). (Likewise the ratio  $R/\eta_m$  (23) as required for the alternate lifetime estimate (19).) Thus from (17) or (19) we obtain

$$\tau_c = \tau_c' \sim \sqrt{2/3} L_0^2 / (\Omega L_s^2) \quad (24)$$

Taking  $L_s = 6$  and  $L_0 = 20$  we find

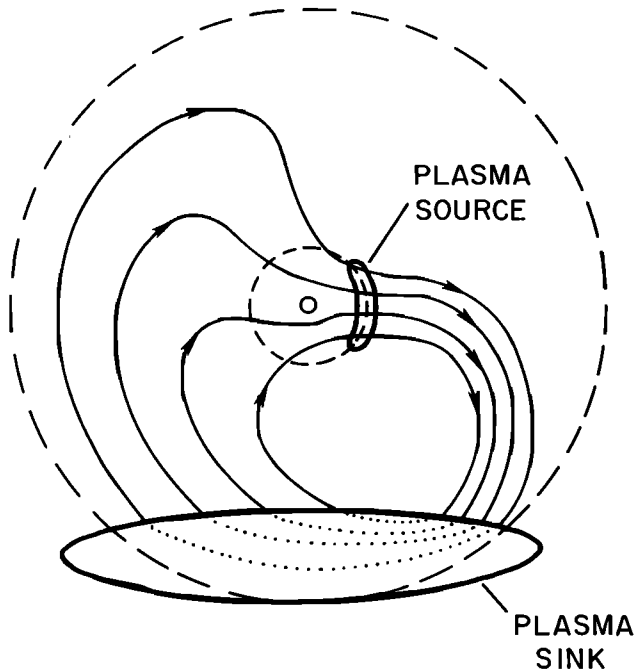


Fig. 2. Sketch of the anticipated pattern of convection in the corotating frame of reference. The asymmetric source of plasma in the Io torus drives an outflow in a restricted range of longitudes; this outflow terminates in the outer magnetosphere ('plasma sink'), probably in the form of a planetary wind in the magnetospheric tail. The return (inward) flow occurs in a broader range of longitudes and involves compression and heating of the low-density plasma therein. Coriolis forces cause a retrograde spiral in the outflow, corresponding to subcorotational azimuthal flow in the nonrotating reference frame. (We expect the flow to exhibit significant time variations so that no simple steady state solution gives a complete representation of the system behavior.)

$$T_c \approx 14 \text{ hours} \quad (25)$$

i.e., an outflow time comparable to a few rotation periods.

This estimate should be regarded as a lower limit because the Coriolis force, which we have neglected here, tends to reduce the radial velocity compared to our estimate by decreasing the effective centrifugal driving force. On the other hand, any magnetic-field-aligned electric field (also neglected here) would tend to increase the radial velocity by reducing the ionospheric drag force. A further, less serious source of error lies in the approximation used above in deriving (15) from (14), which may introduce an error in the radial dependence of  $E_\theta$  in (15); if  $E_\theta$  actually varies as  $r^\alpha$  ( $\alpha > -2$ ), instead of linearly as in (15), then the factor  $\sqrt{3}$  in (22)–(24) would be replaced by  $\sqrt{\alpha + 2}$ . (We have also neglected time variations both in the torus asymmetry and in the resulting convection.)

Nevertheless we regard (24) as a reasonable order-of-magnitude estimate of the outflow time scale. The total convection cycle time would be significantly longer because (a) the return half of the cycle (the inflow) is expected to be slower than the outflow (see our discussion of the convection pattern below), and (b) the initiation of the outflow may be delayed, for example, by a strip of enhanced Jovian ionospheric conductivity connected magnetically to the Io torus and produced by particle precipitation therefrom.

Combining (16) with (22), we have the following estimate of the maximum outflow velocity

$$v_r \approx \Omega R_J L^2 / (\sqrt{6} L_s L_0^2) \sim (2.8 \text{ km/s}) (L/6)^4 \quad (26)$$

or

$$v_r / \Omega r \approx 0.037 (L/6)^3 \quad (27)$$

Note that the neglect of inertial forces (i.e., the assumption  $v_r \ll \Omega r$ ) may become invalid beyond about  $L = 10$ . The convective outflow velocity would attain the local corotation velocity according to (27) at  $L \approx 18$ .

Although we have managed to estimate the outflow velocity and time scale without regard to the value of  $\eta_m$ , this parameter ( $\eta_m$ ) is important in determining the self-consistent values of  $\Sigma$  and  $R$  ((22) and (23) above) and in assessing the power delivered to the magnetosphere through the convection system. The interpretation of Voyager measurements with respect to the value of  $\eta_m$  is, however, somewhat ambiguous, and we will examine this problem in detail, following a short description of the overall convection pattern that we envision.

### CONVECTION PATTERN

Although we have not derived quantitatively the complete convection pattern, we can deduce certain qualitative features of this pattern from the above results and some further reasoning. The most obvious feature is that convection should be outward in the active sector ( $\eta > \eta_0$ ) and inward in the complementary longitude sector ( $\eta < \eta_0$ ). Observations [e.g., *Trafton*, 1980] are consistent with the expectation that the active sector spans about  $100^\circ$  in longitude centered near  $\lambda_{III} = 225^\circ$ , as predicted by the magnetic-anomaly model [*Dessler and Vasyliunas*, 1979, and references therein]. Thus we expect the outflow to commence near Io's orbit in this restricted range of longitudes.

As the plasma moves outward, two effects act to produce deviations from purely radial outflow. First, the (centrifugal) driving force increases as the plasma moves outward; thus the azimuthal current density and hence electric-field strength increase (equations 13b and 15 above) and the outflow is constricted to an even narrower longitude sector. This constriction should continue until inertial forces become important in (1). Second, as the plasma moves outward it lags behind corotation (owing to the Coriolis force) by an amount that increases with increasing radius, this lag becoming significant beyond  $L \sim 20$  [*Hill*, 1979; 1980; *McNutt et al.*, 1979]. The flow lines thus spiral outward with a retrograde sense of rotation as viewed in Jupiter's frame of reference (Figure 2).

Plasma must be lost from the outer portion of the convection system at the same average rate as it is supplied by the source at Io. This loss is illustrated schematically by the intersection of the streamlines with the outer 'plasma sink' boundary in Figure 2. This boundary could, in principal, represent the magnetopause, but arguments have been presented previously to the effect that plasma is lost principally through the planetary spin-periodic opening and closing of field lines on the nightside of Jupiter, forming a planetary wind within the magnetotail [*Hill et al*, 1974b; *Carbary et al.*, 1976]. We therefore expect that outflowing flux tubes from the active sector intersect the open field-line boundary (dashed line in the figure), expel most of their plasma, and then reconnect to form a broad sector of return flow toward Jupiter. This return flow is driven by the fringing electric field in Jupiter's ionosphere produced by the polarization associated with the outward flow in the active sector. Note that the return flow is envisioned to occupy a much broader range of longitude than the outflow and that the speed of this return flow (according to (5)) should therefore be correspondingly less than the outflow

speed. The inflow region should be characterized by less dense, but hotter, plasma than the outflow region; the bulk of the Io plasma is lost in the planetary wind (or other plasma sink), and the remaining plasma is heated by betatron and Fermi compression as it flows back toward Jupiter. We note that neither the plasma sink nor the return flow are steady state phenomena.

We emphasize that the pattern illustrated in Figure 2 is fixed in the corotating frame of reference (the pattern corotates although the plasma itself does not). If the plasma loss takes place primarily in the magnetospheric tail as described by Hill *et al.* [1974b] and Carbary *et al.* [1976], then the 'plasma sink' portion of the outer boundary must be viewed as rotating clockwise (as viewed from the north) with respect to the fixed convection pattern of Figure 2, and the opening and reconnection of the flux tubes occurs once per rotation when the 'plasma sink' (i.e., magnetospheric tail) is in the position shown.

A picture that is qualitatively similar to Figure 2, but with corotation added, has been presented previously by Chen [1977].

#### ESTIMATE OF FLUX-TUBE PLASMA CONTENT

At this point we turn to Voyager observations for an estimate of the flux tube content  $\eta_m$ . McNutt and Belcher [1981] have presented a radial profile of plasma mass density between 5 and 45  $R_J$ , obtained by the plasma experiment on the inbound trajectory of Voyager 1. (Comparisons with the results of other Voyager instruments [Scudder *et al.*, 1981] indicate that the mass density presented by McNutt and Belcher does indeed represent the bulk of the plasma population in this region.) The near-equatorial mass density  $\rho$  is related to the flux-tube content  $\eta$  by

$$\eta \approx 2\rho H_c / B \quad (28)$$

where

$$H_c = (2kT/3m\Omega^2)^{1/2} \quad (29)$$

is the centrifugal scale height [Hill and Michel, 1976], that is, the distance from the centrifugal equator within which the plasma is largely confined. (The centrifugal equator marks the position of centrifugal equilibrium along a field line—see [Hill *et al.*, 1974a; Cummings *et al.*, 1980].) Taking the average ion mass (temperature) to be 22 amu (30 eV) [McNutt and Belcher, 1981], we have  $H_c \approx 0.75 R_J$ .

The field strength  $B$  in (30) refers to the  $z$  component measured at, and perpendicular to, the equator; this component follows the dipole radial dependence rather closely within 45  $R_J$  (although the total off-equatorial field strength does not) [Smith *et al.*, 1974]. Thus we use  $H_c = 0.75 R_J$  and  $B = (0.42/L^3) G$  in (30) to infer  $\eta(r)$  from the profile  $\rho(r)$  published by McNutt and Belcher [1981].

The resulting profile is shown in Figure 3. The connected points within  $r < 10 R_J$  represent simply a low-resolution scaling of the (higher-resolution) plasma data provided by McNutt and Belcher; the points outside 10  $R_J$ , however, have significance as discrete points—each point represents a local maximum of the mass density associated with the quasi-periodic (semidiurnal) variations evident in the data of McNutt and Belcher. These variations presumably are due to the latitudinal excursions of Voyager 1 about the centrifugal (or magnetic) equator owing to the tilt of Jupiter's magnetic dipole axis. Thus only the peak values of  $\rho$  within each semi-

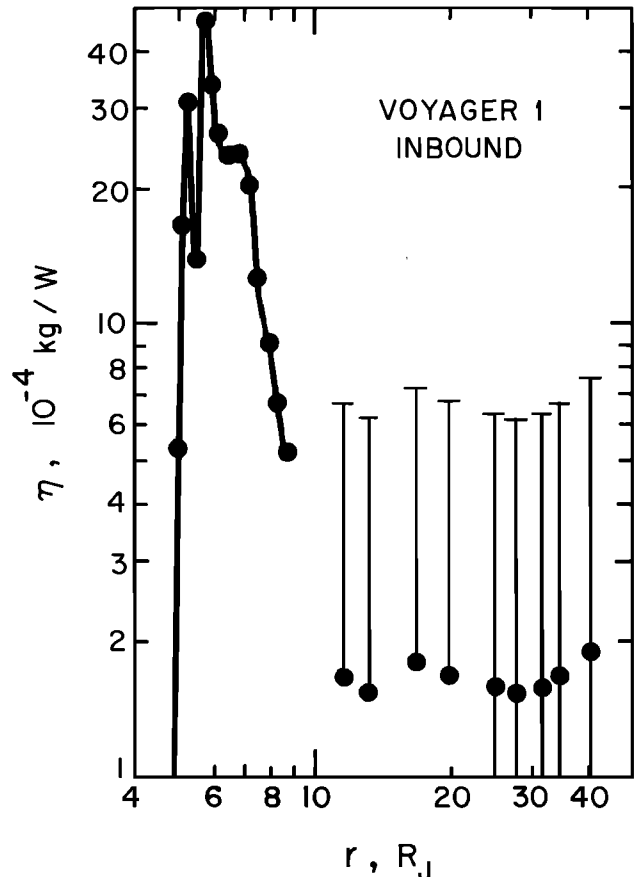


Fig. 3. The flux-tube content (mass per unit magnetic flux) as a function of Jovicentric distance along the Voyager 1 inbound track, calculated from the plasma mass density measurements presented by McNutt and Belcher [1981]. This quantity should be conserved along convection streamlines in the absence of time variations or unexpected loss processes. The large variation between the regions  $r < 10 R_J$  and  $r > 10 R_J$  is taken to indicate that Voyager 1 inbound did not encounter the outflow region beyond 10  $R_J$  (see text and Figure 4 below).

diurnal oscillation are relevant for the evaluation of  $\eta$ , and only these are plotted in Figure 3 (beyond 10  $R_J$ ). (All the data within  $r < 10 R_J$  were taken close to the centrifugal equator and within one-half Jovian rotation, so that any latitude variation here is impossible to distinguish from radial and/or longitudinal variations.) The points beyond 20  $R_J$  in Figure 3 probably represent underestimates of the flux-tube content, for two reasons: (1) the equatorial field strength between 10 and 20  $R_J$  is evidently less than the dipole value by as much as a factor of 2 [Connerney *et al.*, 1981], owing to the ring-current inflation of the field, and (2) the centrifugal scale height (29) may be increased by as much as a factor of 2, owing to ion heating and/or a reduction of the rotation frequency  $\Omega$ . We represent these combined uncertainties in Figure 3 by attaching a factor-of-4 error bar on the positive side of each point beyond 20  $R_J$ . The first effect (ring-current inflation) should diminish and, indeed, reverse at some point because the ring-current inflation produces an enhancement of the equatorial field strength beyond the effective centroid of the ring-current distribution; accordingly we have also attached an indefinite error bar on the negative side of each point beyond 20  $R_J$ .

In spite of these rather large uncertainties in our estimation of flux-tube content, there remains a clear discrepancy in the Voyager data as represented in Figure 3. The quantity plotted

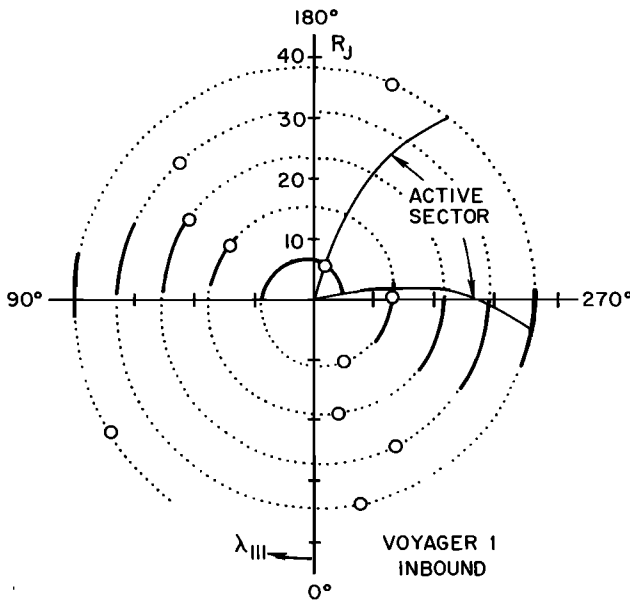


Fig. 4. The Voyager 1 inbound track (dotted curve) is plotted in  $r - \lambda_{III}$  coordinates, showing the locations of expected (solid portions of the curve) and observed (circles) encounters with the equatorially confined plasma distribution. Note that neither the expected nor the actual encounters with the equatorial region occurred in the expected longitude range of the active-sector outflow region beyond  $10 R_J$ .

is flux-tube content ( $\eta$ ), which, according to (7) above, is supposed to be conserved along streamlines. It is clearly not conserved within  $6 R_J \leq r \leq 10 R_J$  in the figure, although it appears to be well conserved in the region sampled outside of  $10 R_J$ . Three possible resolutions of this dilemma have occurred to us: (1) a powerful loss mechanism may actually have depleted the flux tubes between  $6 R_J$  and  $10 R_J$ ; (2) a drastic time variation (an order-of-magnitude increase) in the plasma source flux [cf. Richardson *et al.*, 1980] may have occurred shortly before the Voyager 1 encounter, thus invalidating (7); or (3) Voyager 1 may never have encountered the enhanced density of the outflow region (within a scale height of the centrifugal equator) except within  $r < 10 R_J$ ; i.e. the regions  $r < 10 R_J$  and  $r > 10 R_J$  in Figure 3 are not connected by convection streamlines.

We favor the third explanation for the following reasons:

1. The lifetimes of ions against recombination and against precipitation into Jupiter's atmosphere both exceed by many orders of magnitude the particle residence time estimated above (25), or even the more conservative residence times estimated by other workers, as discussed later. No other effective loss mechanism is evident.

2. The possibility of a drastic time variation cannot be definitively ruled out, although we consider it implausible in view of the lack of evidence for any such variation in remote observations of the torus emissions [Brown *et al.*, 1981]. (The Voyager 2 inbound data presented by McNutt [1980], taken 4 months later, are quite compatible with the  $r > 10 R_J$  data of Figure 3. Voyager 2 did not pass within  $10 R_J$  of Jupiter, and plasma density data for the outbound legs of Voyagers 1 and 2 are not available because of unfavorable detector orientations—see McNutt and Belcher [1981].)

3. The conclusion that Voyager 1 on its inbound orbit did not encounter the active-sector outflow outside of  $10 R_J$  is not only plausible, it is a necessary consequence of our model. We

illustrate this fact in Figure 4 in which the Voyager 1 inbound trajectory is plotted in  $r - \lambda_{III}$  coordinates ( $\lambda_{III}$  is the radio system III (1965) longitude of the spacecraft point). The solid portions of the trajectory indicate intervals when Voyager 1 was within one scale height ( $0.75 R_J$ ) of the centrifugal equator as determined from a centered dipole model of Jupiter's magnetic field tilted  $10.8^\circ$  toward  $\lambda_{III} = 200^\circ$ . On the remainder of the trajectory (dotted portion), Voyager 1 was more than one scale height from the centrifugal equator and thus unable to detect the bulk of the equatorially confined plasma at the given longitude. (If we had used the magnetic equator rather than the centrifugal equator as the hypothetical equilibrium point of the latitudinal mass distribution [cf. Hill *et al.*, 1974b; Goertz, 1976; Cummings *et al.*, 1980], the solid portions of the curve would have been displaced only slightly in longitude, not significantly on the scale of Figure 4.) The circles denote the positions along the trajectory of the local (semi-diurnal) maxima in the plasma mass density data of McNutt and Belcher [1981] (the same points as given in our Figure 3 for  $r > 10 R_J$ , plus the maximum of the torus profile at  $r \approx 6 R_J$ ).

The point we wish to make with Figure 4 is that the actual observed crossings of the plasma sheet (circles in the figure) occurred well outside the predicted longitude sector of the convective outflow. [This is also true, though to a lesser extent, of the expected crossing positions (the solid portions of the trajectory).] The outflow is expected to be confined (at least) within the active sector, which is drawn as a  $60^\circ$  longitude sector centered on  $\lambda_{III} = 230^\circ$  near the torus and spiraling to greater longitudes with increasing radius—the spiral angle is qualitatively sketched in a manner consistent with the observed corotation lag and also consistent with the observed lag between expected and observed plasma-sheet crossings. We therefore conclude that Voyager 1 did not encounter the enhanced density of the outflow sector, which is confined both in longitude (as described above) and in latitude (as described earlier by Hill and Michel [1976] and by Siscoe [1977]), except within  $10 R_J$  distance. The large variations observed within  $10 R_J$  can be interpreted entirely as longitudinal variations (these data were all taken within a scale height of the centrifugal equator, and the maximum occurs in the active sector as expected). Specifically, we propose that the peak value  $\eta_1 \sim 4 \times 10^{-3}$  kg/W observed near ( $r = 6 R_J$ ,  $\lambda_{III} = 200^\circ$ ) applies to the entire symmetry streamline of the outflow region, but that Voyager 1 inbound did not encounter the near-equatorial portion of this outflow streamline beyond  $10 R_J$  because of unfavorable orbit parameters. Thus we would adopt  $\eta_1 \sim 4 \times 10^{-3}$  kg/W for the value of  $\eta_m$  as defined above. A similar analysis of the Voyager 2 inbound data of McNutt [1980] is consistent with the same interpretation, although in this case the semi-diurnal (latitudinal) peaks beyond  $10 R_J$  are less clearly defined and the spacecraft did not approach within  $10 R_J$ .

On the other hand, it is possible that we have been deceived by either (1) an unanticipated plasma loss mechanism or (2) a drastic time variation, as discussed above, such that the more appropriate value for the bulk of the outflow region would be  $\eta_2 \sim 2 \times 10^{-4}$  kg/W, which is characteristic of the values beyond  $10 R_J$  in Figure 3. In the following we shall therefore estimate all parameters depending on  $\eta_m$  in terms of the two possible extreme values,  $\eta_1 \sim 4 \times 10^{-3}$  kg/W and  $\eta_2 \sim 2 \times 10^{-4}$  kg/W.

For example, the self-consistently required values of  $\Sigma$  and  $R$  ((22) and (23) above, respectively) would be

$$\Sigma \sim \begin{cases} 5 \text{ mho} & (\eta = \eta_1) \\ 0.25 \text{ mho} & (\eta = \eta_2) \end{cases} \quad (30)$$

and

$$R \sim \begin{cases} 5 \times 10^{21} \text{ amu/s} & (\eta = \eta_1) \\ 2.6 \times 10^{20} \text{ amu/s} & (\eta = \eta_2) \end{cases} \quad (31)$$

We can compare (30) with the range  $\Sigma \sim 1\text{--}10$  mho computed by R. M. Thorne (private communication, 1980) from the effect of enhanced ionization in the Jovian ionosphere caused by electron precipitation from the Io plasma torus (this enhanced ionization, and the associated enhanced conductivity, would tend to follow the convection outward, i.e., poleward as projected onto Jupiter, within the outflow region).

#### CONVECTION POWER

The convection system provides a specific mechanism for tapping Jupiter's rotational energy to power magnetospheric phenomena. The equatorial ring current of the outflow region (Figure 1), where  $\mathbf{J} \cdot \mathbf{E} < 0$ , converts rotational energy into electromagnetic energy that is largely stored in the outward magnetic-field distortion produced by the current  $\mathbf{J}$ . This energy is consumed both by the compression (and attendant particle acceleration) that occurs in the inflow region and by Joule heating in the ionosphere, both of which regions have  $\mathbf{J} \cdot \mathbf{E} > 0$ .

The rate of this energy conversion is readily estimated [cf. *Dessler, 1980a; Eviatar and Siscoe, 1980*] by considering that mass is transported at the rate  $R(\text{kg/s})$  through the centrifugal potential field  $\omega^2 r$ , where  $\omega \leq \Omega$  is the actual rotation frequency of the plasma. Thus the power delivered is

$$P \approx R \int_{r_{6R}}^{r_m} \omega^2 r dr \quad (32)$$

where  $r_m$  is the outer limit of the outflow region. A reasonable approximation to this integral is obtained [*Hill, 1979*] if we assume  $\omega = \Omega$  for  $L < L_0$  and  $\omega = \Omega (L_0/L)^2$  for  $L > L_0$ , where  $L_0$  ((20) above) is the characteristic distance for corotation breakdown as described above (we assume  $L_0 \leq r_m/R_j$ ). Thus (32) gives

$$P \approx R\Omega^2 R_j^2 L_0^2 \approx \sqrt{3/2} \pi \Omega^3 R_j^4 B_j \eta_m L_0 \quad (33)$$

For the two alternate empirical values  $\eta_1$  and  $\eta_2$  described in the preceding section, the power is

$$\begin{aligned} P_1 &\sim 5.5 \times 10^{15} \text{ W} & (\eta \sim \eta_1) \\ P_2 &\sim 2.7 \times 10^{14} \text{ W} & (\eta \sim \eta_2) \end{aligned} \quad (34)$$

Another relevant parameter is the total electric potential drop  $\Phi_0$  across the outflow region, which represents the rate at which magnetic flux is intercepted by the outflow:

$$\Phi_0 = R/\eta \sim 22 \text{ MV} \quad (35)$$

(independent of the choice of  $\eta$ ). By contrast, the total potential drop associated with an Earthlike solar-wind-driven convection system at Jupiter has been estimated from simple scaling laws as  $\Phi_{sw} \approx 1 \text{ MV}$  [e.g., *Kennel and Coroniti, 1977*]. From this comparison we conclude that solar-wind-induced convection is negligible compared to internally driven convection insofar as radial plasma transport is concerned.

It is interesting to note that the relation (35) establishes the exact equivalence between the volume integral of  $-\mathbf{j} \cdot \mathbf{E}$  over

the outflow region and the alternate form (32) that we have used to estimate the power in the outflow.

The total current associated with the convection system can be obtained by integrating the current density (13b) over the outflow region. A simpler and equivalent method (the equivalence again being established by (35)) is

$$I = P/\Phi \sim \begin{cases} 2.5 \times 10^8 \text{ A} & (\eta \sim \eta_1) \\ 1.25 \times 10^7 \text{ A} & (\eta \sim \eta_2) \end{cases} \quad (36)$$

Using similar parameters, *Dessler [1980b]* has estimated that roughly  $5 \times 10^6 \text{ A}$  flows through the torus itself; the remainder of the current is distributed through the much larger volume of the convective outflow region. (When comparing the results of *Dessler [1980b]* with those of the present paper, the reader should note the different definitions of the symbol  $\sigma$ .)

#### DISCUSSION

The phenomenon of internally driven convection is implicit in most discussions of large-scale radial transport in Jupiter's magnetosphere, and especially in any discussion of a planetary wind outflow. It has usually been assumed, either implicitly or explicitly, that the internally driven convection consists of small-scale eddies whose motion is stochastic and longitudinally symmetric and therefore describable in terms of a radial diffusion equation. Such models have been developed under the assumption that the eddy convection is driven either by Jovian atmospheric winds [*Brice and McDonough, 1973*] or by the interchange instability of the Io torus mass distribution [*Siscoe and Summers, 1981*].

The convection system described here, as driven by the longitudinal asymmetry of the Io torus, differs in two important respects from these radial diffusion models: (1) it is characterized by a systematic pattern with outflow in the active sector and inflow in the complementary longitude sector; this pattern corotates with Jupiter, although the plasma may not; and (2) it is considerably faster, transporting material outward on a time scale of a few rotation periods, compared to  $\sim 1$  year for atmospherically driven diffusion [*Coroniti, 1974*] or  $\sim 45$  days for centrifugally driven interchange diffusion [*Siscoe and Summers, 1981*]. (It should be noted, however, that the estimate of *Siscoe and Summers* would be comparable to our estimate if our larger estimate of  $R$  (31) were used in their analysis. Their method of estimating the time scale is essentially equivalent to our second method (19) above.) The return (inflow) half of the convection cycle should occur somewhat more slowly, requiring perhaps several Jovian rotations.

Our convection pattern (Figure 2) should be considered a gross time-average pattern upon which may be superimposed a noise component associated with eddy convection of the type described by *Siscoe and Summers*. In our large-scale pattern the flux-tube content ( $\eta$ ) is conserved, and the mass distribution is therefore marginally stable against flux-tube interchange motions [see *Hill, 1976*, and references therein]. It is likely that the flux-tube interchange instability as described by *Siscoe and Summers* initiates the plasma outflow (particularly when the Io plasma source is time variable), and that our convection pattern represents the steady state toward which the system evolves, i.e., the saturation state of the centrifugal interchange instability.

The corotating convection pattern that we have proposed has a number of observable consequences. The most obvious prediction is that the radial plasma velocity component

should vary systematically with Jovian longitude (but with time-dependent fluctuations). This prediction can in principle be checked against Voyager plasma flow measurements, although there appears to be some difficulty in deriving information on the radial velocity components from the Voyager plasma data [see, for example, *McNutt and Belcher, 1981*].

Other potentially observable effects include those of the associated Birkeland currents [*Dessler, 1980b*] and of the compression that takes place in the inflow region opposite the active sector [*Dessler et al., 1981*]. For example, *Dessler [1980b]* has suggested that the Birkeland currents associated with the asymmetric ring current (Figure 1) are associated with the decametric and/or kilometric radio emissions which are known to be highly structured in Jovian longitude. Further, *Dessler et al. [1981]* have attributed the observed Lya 'hydrogen bulge' at a fixed Jovian longitude opposite that of the active sector [*Sandel et al., 1980*] to the precipitation of hot electrons in the inflow sector of the corotating convection system.

Other experimental tests capable of distinguishing between the corotating convection model described here and the radial diffusion models prevalent in the literature will no doubt become apparent. The fundamental distinction is the extent to which the magnetospheric plasma mass distribution and the resultant radial transport properties depend on Jovian longitude.

Saturn's magnetosphere also exhibits spin-periodic radio emissions [*Kaiser et al., 1980*], in spite of the negligible tilt angle between its spin axis and magnetic dipole axis [*Smith et al., 1980; Ness et al., 1980*]. This spin periodicity may reflect the existence of a corotating plasma asymmetry in Saturn's magnetosphere, in which case the corotating convection system described above may apply also to Saturn.

#### APPENDIX

Here we show that the current-continuity equation

$$\nabla \cdot \mathbf{j} = 0 \quad (\text{A1})$$

implies equation (10) of the text when applied to both the equatorial and Jovian ionospheric ends of a field line.

Integrating (A1) across the equatorial current sheet yields

$$2j_{\parallel}^e + \frac{1}{r} \frac{\partial}{\partial r} (rJ_r^e) + \frac{1}{r} \frac{\partial}{\partial \theta} (J_{\theta}^e) = 0 \quad (\text{A2})$$

where superscript 'e' denotes the equatorial end of the field line and  $j_{\parallel}^e$  is defined positive for currents flowing away from the equatorial plane toward Jupiter. (For simplicity we will assume a spin-aligned dipole magnetic field so that  $j_{\parallel}$  flows symmetrically to northern and southern hemispheres.)

The Birkeland current density  $j_{\parallel}$  is (by definition) proportional to the field strength  $B$  as it flows along the field toward Jupiter's ionosphere (it is assumed that no significant transverse currents flow except at the equatorial and ionospheric ends of the field line). Thus

$$j_{\parallel}^i = j_{\parallel}^e B^i / B^e = j_{\parallel}^e (4 - 3 \sin^2 \xi)^{1/2} / L^3 \quad (\text{A3})$$

where superscript 'i' denotes the Jovian ionospheric end of the field line (either northern or southern hemisphere), and  $\xi$  is the polar angle (colatitude) of a Jupiter-centered spin-aligned spherical  $(R, \xi, \theta)$  coordinate system, i.e.,

$$\sin^2 \xi = 1/L \quad (\text{A4})$$

At the Jovian ionospheric end of the field line, (A1) can be

integrated through the Pedersen-conducting layer of the ionosphere to give

$$-j_{\parallel}^i |B_R^i / B^i| + \frac{1}{R_j \sin \xi} \frac{\partial}{\partial \xi} (J_{\xi}^i \sin \xi) + \frac{1}{R_j \sin \xi} \frac{\partial}{\partial \theta} (J_{\theta}^i) = 0 \quad (\text{A5})$$

For the surface dipole field,

$$|B_R / B| = 2 |\cos \xi| / (4 - 3 \sin^2 \xi)^{1/2}$$

We assume that Jupiter's ionosphere has uniform Pedersen conductivity  $\Sigma$  so that

$$\mathbf{J}^i = \Sigma \mathbf{E}^i \quad (\text{A6})$$

Combining (A3) through (A6) yields

$$(2 R_j / \Sigma) L^{3/2} (1 - 1/L)^{1/2} j_{\parallel}^e = \frac{\partial}{\partial \xi} (E_{\xi}^i \sin \xi) + \frac{\partial}{\partial \theta} (E_{\theta}^i) \quad (\text{A7})$$

The electric-field components can be mapped from the ionosphere to the equatorial plane according to

$$E_{\theta}^e = E_{\theta}^i L^{-3/2} \quad (\text{A8})$$

$$E_r^e = -\frac{1}{2} E_{\xi}^i L^{-3/2} (1 - 1/L)^{-1/2} \quad (\text{A9})$$

and from (A4) we have

$$\frac{\partial}{\partial \xi} = -2L^{3/2} (1 - 1/L)^{1/2} \frac{\partial}{\partial L} \quad (\text{A10})$$

Combining (A2) with (A7) through (A10) yields

$$\begin{aligned} \frac{\partial}{\partial r} (rJ_r^e) + \frac{\partial}{\partial \theta} (J_{\theta}^e) = & -4 \Sigma \frac{\partial}{\partial L} [L(1 - 1/L)^{1/2} E_r^e] \\ & - \Sigma (1 - 1/L)^{1/2} \frac{\partial}{\partial \theta} (E_{\theta}^e) \end{aligned} \quad (\text{A11})$$

If we adopt the approximation

$$(1 - 1/L)^{1/2} \approx 1 \quad (\text{A12})$$

(good for  $L \geq 6$ ) and suppress the superscript 'e,' (A11) becomes (10) of the text.

*Acknowledgments.* We are grateful to V. M. Vasylunas for helpful comments and discussions. This work was supported in part by the Atmospheric Research Section of the National Science Foundation under grants ATM78-21767 and ATM80-19425.

#### REFERENCES

- Brice, N. M., and T. R. McDonough, Jupiter's radiation belts, *Icarus*, **18**, 206, 1973.
- Broadfoot, A. L., B. R. Sandel, D. E. Shemansky, J. C. McConnell, G. R. Smith, J. B. Holberg, S. K. Atreya, T. M. Donahue, D. F. Strobel, and J. L. Bertaux, Overview of the Voyager ultraviolet spectrometry results through Jupiter encounter, *J. Geophys. Res.*, **10**, 8259, 1981.
- Brown, R. A., C. B. Pilcher, and D. F. Strobel, Photometric study of the Io torus, in *Physics of the Jovian Magnetosphere*, edited by A. J. Dessler, chap. 6, in press, Cambridge University Press, New York, 1981.
- Carbary, J. F., T. W. Hill, and A. J. Dessler, Planetary spin period acceleration of particles in the Jovian magnetosphere, *J. Geophys. Res.*, **81**, 5189, 1976.
- Chen, C.-K., Topics in planetary plasmaspheres, Ph.D. thesis, Univ. of Calif., Los Angeles, 1977.



- Connerney, J. E. P., M. H. Acuña, and N. F. Ness, Modeling the Jovian current sheet and inner magnetosphere, *J. Geophys. Res.*, in press, 1981.
- Coroniti, F. V., Energetic electrons in Jupiter's magnetosphere, *Astrophys. J. Suppl.*, **244**, 27, 261, 1974.
- Cummings, W. D., A. J. Dessler, and T. W. Hill, Latitudinal oscillations of plasma within the Io torus, *J. Geophys. Res.*, **85**, 2108, 1980.
- Dessler, A. J., Mass-injection rate from Io into the Io plasma torus, *Icarus*, **44**, 291, 1980a.
- Dessler, A. J., Corotating Birkeland currents in Jupiter's magnetosphere: An Io plasma-torus source, *Planet. Space Sci.*, **28**, 781, 1980b.
- Dessler, A. J., and T. W. Hill, High-order magnetic multipoles as a source of gross asymmetry in the distant Jovian magnetosphere, *Geophys. Res. Lett.*, **2**, 567, 1975.
- Dessler, A. J., and T. W. Hill, Jovian longitudinal control of Io-related radio emissions, *Astrophys. J.*, **227**, 664, 1979.
- Dessler, A. J., and V. M. Vasylunas, The magnetic anomaly model of the Jovian magnetosphere: Predictions for Voyager, *Geophys. Res. Lett.*, **6**, 37, 1979.
- Dessler, A. J., B. R. Sandel, and S. K. Atreya, The Jovian hydrogen bulge: Evidence for co-rotating magnetospheric convection, *Planet. Space Sci.*, **29**, 215, 1981.
- Eviatar, A., and G. L. Siscoe, Limit on rotational energy available to excite Jovian aurora, *Geophys. Res. Lett.*, **7**, 1085, 1980.
- Fillius, R. W., and P. Knickerbocker, The phase of the 10-hour modulation in the Jovian magnetosphere (Pioneers 10 and 11), *J. Geophys. Res.*, **84**, 5763, 1979.
- Goertz, C. K., The current sheet in Jupiter's magnetosphere, *J. Geophys. Res.*, **81**, 3368, 1976.
- Hill, T. W., Interchange stability of a rapidly rotating magnetosphere, *Planet. Space Sci.*, **24**, 1151, 1976.
- Hill, T. W., Inertial limit on corotation, *J. Geophys. Res.*, **84**, 6554, 1979.
- Hill, T. W., Corotation lag in Jupiter's magnetosphere: A comparison of observation and theory, *Science*, **207**, 301, 1980.
- Hill, T. W., and A. J. Dessler, Longitudinal asymmetry of the Jovian magnetosphere and the periodic escape of energetic particles, *J. Geophys. Res.*, **81**, 3383, 1976.
- Hill, T. W., A. J. Dessler, and F. C. Michel, Configuration of the Jovian magnetosphere, *Geophys. Res. Lett.*, **1**, 3, 1974a.
- Hill, T. W., and F. C. Michel, Heavy ions from the Galilean satellites and the centrifugal distortion of the Jovian magnetosphere, *J. Geophys. Res.*, **81**, 4561, 1976.
- Hill, T. W., J. F. Carbary, and A. J. Dessler, Periodic escape of relativistic electrons from the Jovian magnetosphere, *Geophys. Res. Lett.*, **1**, 333, 1974b.
- Kaiser, M., M. Desch, J. Alexander, J. Thieman, J. Pearce, J. Warwick, B. Pedersen, T. Carr, and J. Schauble, Planetary radio astronomy, paper presented at the Fall AGU Meeting, San Francisco, Calif., December 1980.
- Kennel, C. F., and F. V. Coroniti, Jupiter's magnetosphere, *Ann. Rev. Astron. Astrophys.*, **15**, 389, 1977.
- McNutt, R. L., Jr., *The Dynamics of the Low Energy Plasma in the Jovian Magnetosphere*, Ph.D. thesis, MIT, Cambridge, Mass., 1980.
- McNutt, R. L., Jr., and J. W. Belcher, Positive ion observations in the middle magnetosphere of Jupiter, *J. Geophys. Res.*, in press, 1981.
- McNutt, R. L., Jr., J. W. Belcher, J. D. Sullivan, F. Bagenal, and H. S. Bridge, Departure from rigid corotation of plasma in Jupiter's dayside magnetosphere, *Nature*, **280**, 803, 1979.
- Ness, N. F., M. Acuña, K. Behannon, L. Burlaga, J. Connerney, R. Lepping, and F. Neubauer, Magnetic field investigation, paper presented at the Fall AGU Meeting, San Francisco, Calif., December 1980.
- Pilcher, C. B., and J. S. Morgan, The distribution of [SII] emission around Jupiter, *Astrophys. J.*, **238**, 375, 1980.
- Richardson, J. D., G. L. Siscoe, F. Bagenal, and J. D. Sullivan, Time dependent plasma injection by Io, *Geophys. Res. Lett.*, **7**, 37, 1980.
- Sandel, B. R., A. L. Broadfoot, and D. F. Strobel, Discovery of a longitudinal asymmetry in the H Lyman-alpha brightness of Jupiter, *Geophys. Res. Lett.*, **7**, 5, 1980.
- Scudder, J. D., E. C. Sittler, Jr., and H. S. Bridge, Survey of the plasma electron environment of Jupiter: A view from Voyager, *J. Geophys. Res.*, in press, 1981.
- Siscoe, G. L., On the equatorial confinement and velocity space distribution of satellite ions in Jupiter's magnetosphere, *J. Geophys. Res.*, **82**, 1641, 1977.
- Siscoe, G. L., and D. Summers, Centrifugally driven diffusion of Io-genic plasma, *J. Geophys. Res.*, in press, 1981.
- Smith, E. J., L. Davis, Jr., D. E. Jones, P. J. Coleman, Jr., D. S. Colburn, P. Dyal, C. P. Sonett, and A. M. A. Frandsen, The planetary magnetic field and magnetosphere of Jupiter: Pioneer 10, *J. Geophys. Res.*, **79**, 3501, 1974.
- Smith, E. J., L. Davis, Jr., D. E. Jones, P. J. Coleman, Jr., D. S. Colburn, P. Dyal, and C. P. Sonett, Saturn's magnetic field and magnetosphere, *Science*, **207**, 407, 1980.
- Trafton, L., The Jovian SII torus: Its longitudinal asymmetry, *Icarus*, **42**, 111, 1980.
- Trauger, J. T., G. Münch, and F. L. Roesler, A study of the Jovian [SII] nebula at high spectral resolution, *Astrophys. J.*, **236**, 1035, 1980.
- Vasylunas, V. M., Mathematical models of magnetospheric convection and its coupling to the ionosphere, in *Particles and Fields in the Magnetosphere*, edited by B. M. McCormac, p. 60, D. Reidel, Dordrecht, Holland, 1970.
- Vasylunas, V. M., Modulation of Jovian interplanetary electrons and the longitude variation of decametric emissions, *Geophys. Res. Lett.*, **2**, 87, 1975.
- Vasylunas, V. M., A mechanism for plasma convection in the inner Jovian magnetosphere (abstract), STP Symposium, Book of Abstracts, Innsbruck, Austria, June 1978.
- Vasylunas, V. M., and A. J. Dessler, The magnetic anomaly model of the Jovian magnetosphere: A post-Voyager assessment, *J. Geophys. Res.*, **86**, in press, 1981.
- Wolf, R. A., Effects of ionospheric conductivity on convective flow of plasma in the magnetosphere, *J. Geophys. Res.*, **75**, 4677, 1970.

(Received December 24, 1980;  
revised April 21, 1981;  
accepted May 7, 1981.)